

Hexagonal Warping Control of Exceptional Points in Topological Insulator–Ferromagnetic Heterojunctions

Md Afsar Reja^{1,*} and Awadhesh Narayan^{1,†}

¹*Solid State and Structural Chemistry Unit, Indian Institute of Science, Bangalore 560012, India*

(Dated: January 13, 2026)

Exceptional points (EPs) are non-Hermitian degeneracies, where both eigenvalues and eigenvectors coalesce, which are fundamentally distinct from their Hermitian counterparts. In this study, we investigate the influence of hexagonal warping on EPs emerging at the interfaces between topological insulators and ferromagnets. We demonstrate that the presence of the warping term plays a crucial role in determining the locations of the EPs. Furthermore, we show that the number as well as the positions of EPs emerging at such junctions can be tuned by an applied magnetic field. Our results establish a realistic and experimentally accessible platform for exploring non-Hermitian physics in topological insulator-ferromagnet junctions.

I. INTRODUCTION

Non-Hermitian (NH) systems exhibit a broad range of novel phenomena, including EPs, the non-Hermitian skin effect, and extended classes of topological phases, to name a few [1–9]. A key feature of non-Hermitian systems is the presence of EPs – degeneracies at which both eigenvalues and eigenvectors coalesce together [10, 11]. These are distinct from Hermitian degeneracies, where only the eigenvalues coincide while the eigenvectors remain orthogonal. EPs are connected to a wide range of intriguing phenomena, spanning both theory and practical applications. These include NH topological phases characterized by the winding of eigenvalues and eigenvectors around the EPs [6, 12, 13], potentially enhanced sensing capabilities [14], exceptional optical microcavities [15], and directional lasing technologies [16]. Experimentally, EPs have been realized in a variety of platforms, including optics, photonics, electrical circuits, and acoustic systems [17–23]. Recently, appearance of EPs and their extended versions has been investigated theoretically in heterojunctions composed of unconventional quantum materials and ferromagnets [24–29].

Topological insulators (TIs) have been a central focus in condensed matter physics over the past few decades due to their rich theoretical foundations as well as potential technological applications [30, 31]. One of the intriguing properties of topological insulators is the emergence of snowflake-shaped Fermi surface states, in contrast to the usual circular Fermi surface [32, 33]. The underlying crystal symmetry gives rise to this distinctive Fermi surface geometry, which can be captured by a cubic-in-momentum k^3 hexagonal warping term [34–36]. The role of hexagonal warping effects has previously been explored in various contexts, including optical conductivity [37], circular dichroism [38], nonlinear Hall

effects [39], multi-Weyl semimetals [40], and transport properties [41, 42].

In this work, we investigate the role of hexagonal warping in the emergence of NH phenomena at a TI–ferromagnet (FM) junction. We find that the hexagonal warping leads to unique effects on the EPs. The positions of the EPs directly reflect the symmetry imposed by the hexagonal warping. Furthermore, we propose and demonstrate that the EP locations can be tuned by an applied magnetic field and can even be annihilated through field control. We complement our analytical results for the junctions by means of numerical characterization of the NH degeneracies. Our findings establish TI–FM heterostructures, with hexagonally warped surface states, as a versatile and experimentally

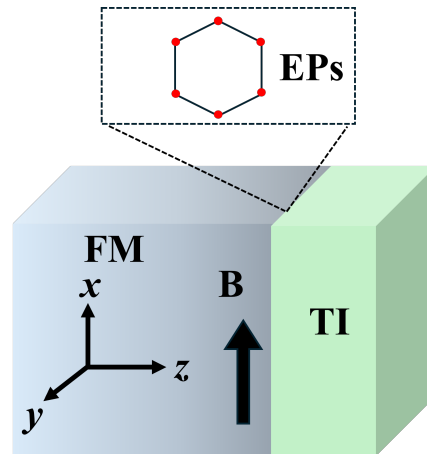


FIG. 1. **Schematic of the proposed topological insulator-ferromagnet junction.** The junction is formed at $z = 0$, while the region $z < 0$ represents the FM lead which is in contact with a TI film (extending for $z > 0$). The red dots in the inset denote the emergent EPs, which follow the symmetry imposed by the hexagonal warping term. The thick black arrow denotes the direction of the externally applied magnetic field, which serves as a tuning parameter for controlling the position and evolution of the EPs.

* afsarmd@iisc.ac.in

† awadhesh@iisc.ac.in

accessible platform for exploring NH physics.

II. SETUP OF TOPOLOGICAL INSULATOR-FERROMAGNET JUNCTION

We consider a TI coupled to a semi-infinite FM lead, as illustrated in Fig. 1. The interface is located at $z = 0$, with the FM lead occupying the region $z < 0$. The resulting junction is treated as an open quantum system and is described by the following effective Hamiltonian,

$$\tilde{H} = H + \Sigma_L. \quad (1)$$

Here, H denotes the Hamiltonian of the TI (introduced below), while Σ_L is the self-energy induced by the semi-infinite FM lead. Within the wide-band approximation, the self-energy is independent of both momentum and frequency and can be evaluated analytically as [24, 43–45],

$$\Sigma_L = -i\Gamma\sigma_0 - i\gamma\sigma_z, \quad (2)$$

where $\Gamma = \frac{\Gamma_+ + \Gamma_-}{2}$, $\gamma = \frac{\Gamma_+ - \Gamma_-}{2}$, and $\Gamma_{\pm} = \pi|t'|^2\rho_{\pm}^L$. Here $\rho_{\pm}^L = \frac{1}{t'\pi}\sqrt{1 - (\frac{\mu_L \pm m}{2t_z})^2}$. The quantities ρ_{\pm}^L represent the surface density of states of the lead for the spin-up and spin-down channels, respectively. The parameter t' represents the hopping amplitude between the FM lead and the TI. Here, σ_x , σ_y , and σ_z are the Pauli matrices, and σ_0 represents the 2×2 identity matrix. The parameter t_z corresponds to the hopping amplitude along the z -direction within the lead. The quantity μ_L is the chemical potential of the lead, while m characterizes the intrinsic magnetization of the FM lead. The coupling to the lead makes the effective Hamiltonian of the junction display an NH character through the imaginary component of the self-energy. We next investigate the exceptional physics at this proposed junction.

III. EMERGENCE OF EXCEPTIONAL POINTS AT TOPOLOGICAL INSULATOR-FERROMAGNET JUNCTION

As we discussed, we consider a TI–FM junction. Importantly, for the TI, we consider a hexagonally-warped surface state. This is described by the following Hamiltonian proposed by Fu [34],

$$H = \alpha(-k_y\sigma_x + k_x\sigma_y) + \lambda(k_x^3 - 3k_xk_y^2)\sigma_z. \quad (3)$$

The first term represents the linear-in-momentum term with a Fermi velocity α , with $k_x - k_y$ being the in-plane

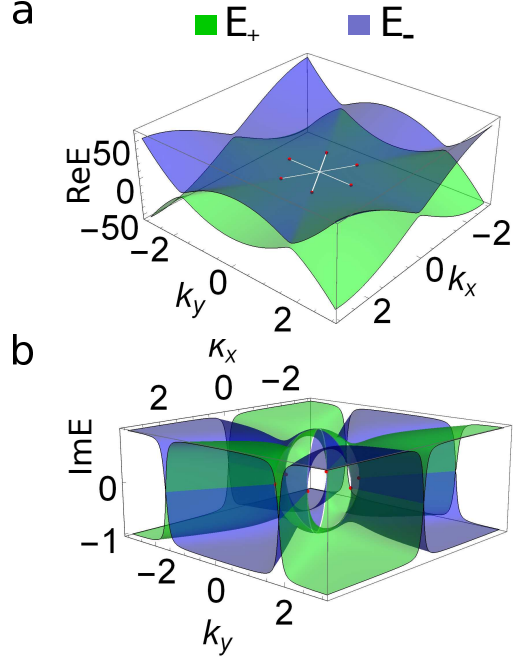


FIG. 2. **Complex band diagram of the junction.** The (a) real and (b) imaginary parts of the energy for the TI-FM junction. The two bands are presented in green and blue colors. Note that both the real and the imaginary parts of the eigenvalues coalesce at the red points, indicating the presence of six EPs which exhibit a hexagonal symmetry. Here, we choose $\lambda = 1$, $\alpha = 1$, $\gamma = 1$, $B_x = 0$.

momenta. The second term corresponds to the hexagonal warping with strength λ . The warping term is invariant under three-fold rotations and plays an essential role to accurately describe the Fermi surfaces of rhombohedral bismuth based topological insulators [34, 35].

Including the self-energy of the FM lead, the complete junction can be represented by the following effective NH Hamiltonian,

$$\begin{aligned} \tilde{H} = H + \Sigma_L \\ = \alpha(-k_y\sigma_x + k_x\sigma_y) + \lambda(k_x^3 - 3k_xk_y^2)\sigma_z \\ + \Sigma_L + B_x\sigma_x. \end{aligned} \quad (4)$$

Here, Σ_L is the self energy term given by Eq. 2 and B_x is an externally applied magnetic field along the x direction (Fig. 1). This NH Hamiltonian can be expressed in the form $\tilde{H} = \epsilon_0 + \mathbf{d} \cdot \boldsymbol{\sigma}$, where $\epsilon_0 = -i\Gamma$, $\epsilon_0 \in \mathbb{C}$ and the complex vector $\mathbf{d} = \mathbf{d}_R + i\mathbf{d}_I$, with $\mathbf{d}_R, \mathbf{d}_I \in \mathbb{R}^3$. For our specific case, the real part is given by $\mathbf{d}_R = (-\alpha k_y + B_x, \alpha k_x, \lambda(k_x^3 - 3k_xk_y^2))$, and the imaginary part is $\mathbf{d}_I = (0, 0, -\gamma)$. The complex energy eigenvalues can be expressed in the form, $E_{\pm} = \epsilon_0 \pm \sqrt{\mathbf{d}_R^2 - \mathbf{d}_I^2 + 2i\mathbf{d}_R \cdot \mathbf{d}_I}$. NH degeneracies occur when the conditions $\mathbf{d}_R^2 = \mathbf{d}_I^2$ and $\mathbf{d}_R \cdot \mathbf{d}_I = 0$ are satisfied simultaneously. For the TI-FM junction with hexagonal warping, the degeneracy conditions read,

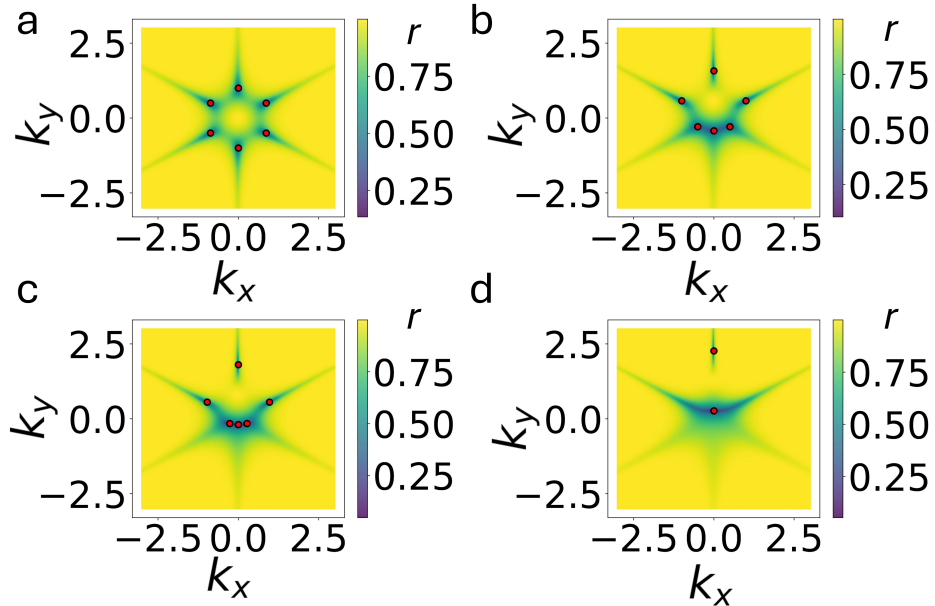


FIG. 3. Magnetic-field tuning of exceptional points. Evolution of the EP positions for different magnetic field values (a) $B_x = 0.0B_c$, (b) $B_x = 0.5B_c$, (c) $B_x = 0.7B_c$, and (d) $B_x = 1.1B_c$. The EPs are shown by red dots, while the phase rigidity is plotted in color (darker colors representing lower values of phase rigidity). As the magnetic field increases, the EPs move in momentum space, and above the critical field, B_c , four EPs annihilate, leaving behind two remanent EPs. The applied field also breaks the underlying hexagonal symmetry arising from the warping term. Here, we choose $\lambda = 1$, $\alpha = 1$, $\gamma = 1$.

$$\gamma^2 = (-\alpha k_y + B_x)^2 + (\alpha k_x)^2 + \lambda^2(k_x^3 - 3k_x k_y^2)^2, \quad (5)$$

$$\gamma \lambda (k_x^3 - 3k_x k_y^2) = 0. \quad (6)$$

Solving these equations, we find that NH degeneracies emerge in the TI–FM junction at the following locations in the k_x – k_y plane,

$$(0, \frac{B_x \pm \gamma}{\alpha}) \quad \text{and} \quad \left(\pm \sqrt{3} \frac{B_x \pm \sqrt{4\gamma^2 - 3B_x^2}}{4\alpha}, \frac{B_x \pm \sqrt{4\gamma^2 - 3B_x^2}}{4\alpha} \right).$$

In general, a total of six EPs appear. We note that the EP locations do not depend explicitly on the hexagonal warping strength, λ . However the hexagonal warping term plays a crucial role in formation of the exceptional degeneracies through the eigenvectors, as we will see. For the rest of our analysis, unless specified otherwise, we set $\lambda = 1$, $\alpha = 1$, $\Gamma = 0$, and $\gamma = 1$. To confirm that the degeneracies are indeed EPs, we plot the real and imaginary parts of the eigenvalues in Fig. 2(a) and (b), respectively, for zero magnetic field, $B_x = 0$. The red dots mark the coalescence of the eigenvalues. Both real and imaginary parts of the energy eigenvalues coalesce at these points, thereby confirming the presence of EPs.

To further establish the coalescence of eigenvectors at these points, we evaluate the phase rigidity, r , as [10]

$$r = \frac{\langle \Psi_L | \Psi_R \rangle}{\langle \Psi_R | \Psi_R \rangle}, \quad (7)$$

where Ψ_L and Ψ_R denote the left and right eigenvectors, respectively. For an NH Hamiltonian, the Hilbert space is spanned by both left and right eigenstates [46], which are generally distinct, in contrast to the Hermitian case. Their orthogonality is established via a biorthogonal normalization, defined by $\langle \Psi_L^m | \Psi_R^n \rangle = \delta_{mn}$. At an EP, the left and right eigenstates become mutually orthogonal, signaling the simultaneous coalescence of both eigenvalues and eigenvectors. Consequently, the phase rigidity vanishes near an exceptional degeneracy ($r \rightarrow 0$) and approaches unity away from it. In Fig. 3(a), we plot the phase rigidity, r , across the k_x – k_y plane. We note that it forms a hexagonal pattern with $r \rightarrow 0$ at six discrete points. These are exactly our analytically obtained positions of the EPs (marked by the red dots), indicating the coalescence of eigenstates at these points. This hexagonal symmetry of the EPs is a direct consequence of the hexagonal warping term. We next show how these can be tuned by the means of a magnetic field.

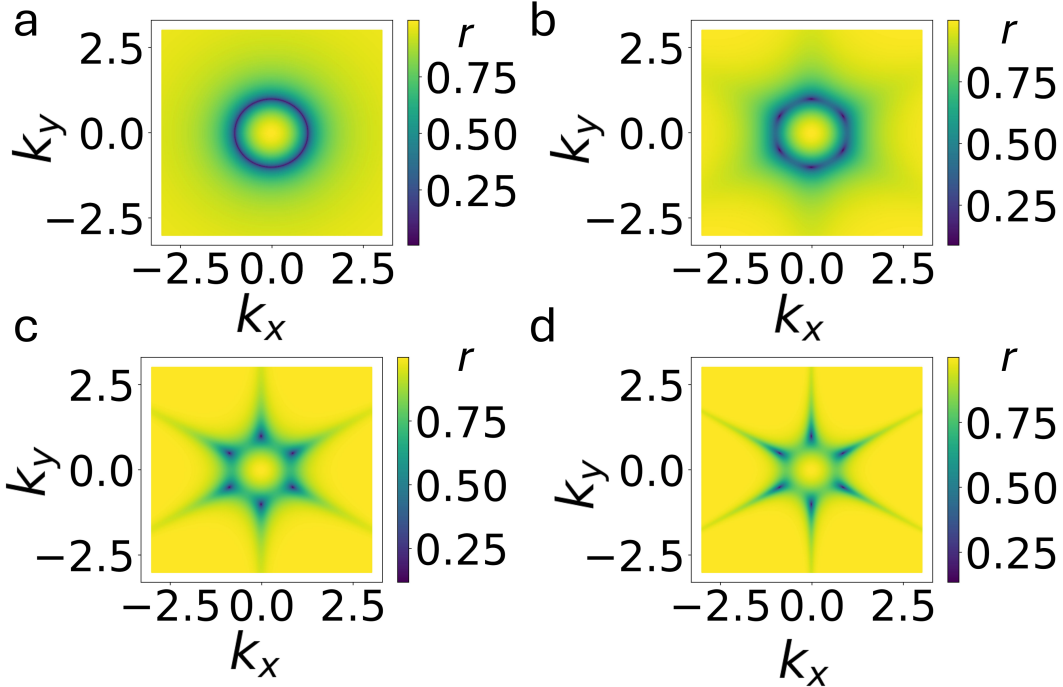


FIG. 4. **Role of hexagonal warping in shaping exceptional degeneracies.** The phase rigidity in the $k_x - k_y$ plane with (a) $\lambda = 0.0$, (b) $\lambda = 0.1$, (c) $\lambda = 0.5$, and (d) $\lambda = 1.0$. At zero hexagonal warping, an exceptional ring is formed centered at the origin. Increasing λ drives the splitting of the exceptional ring into discrete EPs, reflecting the underlying hexagonal symmetry of the warping term. The EPs are robust to the strength of the hexagonal warping. Here, we choose $\alpha = 1, \gamma = 1, B_x = 0$.

IV. TUNING EXCEPTIONAL POINTS WITH A MAGNETIC FIELD

To study the magnetic-field control of the emergent EPs, we consider applying an in-plane magnetic field B_x along the interface, as illustrated in the schematic shown in Fig. 1. Notably, such a magnetic field allows delicate control over the positions of the emergent EPs. First, from our analytical expressions for the EP locations, we find that four of the EPs annihilate at the critical field $B_c = \sqrt{\frac{4}{3}}\gamma$. This corresponds to the square root term in the location of the EPs vanishing. We monitor the evolution of the EPs with increasing magnetic field by means of the phase rigidity. The phase rigidity in the $k_x - k_y$ plane is plotted for a range of B_x values in Fig. 3(a)-(d). As we previously discussed, in the absence of a magnetic field there are six EPs. As the field strength is increased, we find that, among the six EPs, two move towards positive k_y direction on the $k_x = 0$ line, while the remaining four contract toward the origin. We also note that a finite B_x breaks the hexagonal symmetry of the EP positions. For magnetic fields exceeding B_c , only two EPs survive, which are located along the $k_x = 0$ line, as shown in Fig. 3(d). Applying the magnetic field along the y -direction leads to a qualitatively similar annihilation and motion of the EPs. Overall, we find that the interplay of the hexagonal

warping and a magnetic field leads to a robust control over the EPs.

V. SHAPING THE NON-HERMITIAN DEGENERACIES WITH THE WARPING TERM

Next, we investigate the role of the strength of the warping term on the emergent EPs. We begin with $\lambda = 0$, corresponding to the absence of the warping term. In this case, an exceptional ring is formed, where both the eigenvalues and eigenvectors coalesce along a closed ring, as shown in Fig. 4(a). This behavior is analogous to the scenario discussed in Ref. [3], where the addition of an imaginary term proportional to σ_z in a Dirac Hamiltonian leads to the formation of an exceptional ring. We now vary the warping strength and monitor the phase rigidity in the $k_x - k_y$ plane, as shown in Fig. 4(b)-(d), corresponding to $\lambda = 0.1, 0.5$, and 1 , respectively. We find that, for all finite values of λ , the exceptional ring fragments into six EPs. As the warping strength increases, the EPs remain settled at the vertices of a hexagon, reflecting the underlying symmetry imposed by the warping term. As such, the EPs are robust to the strength of the hexagonal warping. We note that the phase rigidity around the EPs is modulated by the warping strength, with the con-

tours in Fig. 4(b)-(d) becoming sharper as λ is increased.

VI. SUMMARY AND OUTLOOK

We have studied the emergence of EPs at a TI-FM heterojunction, where the warping term plays crucial role in shaping the NH degeneracies. We show that the positions as well as the number of the arising EPs can be tuned by an applied magnetic field. Moreover, the EP locations inherit the hexagonal symmetry and are robust to the strength of the warping term of the TI surface state. The prototypical topological material Bi_2Te_3 , with its hexagonally warped surface states will be a suitable avenue for exploring our predictions [32, 36]. Tuning the Fermi level by gating or doping could allow control over the degree of warping. Furthermore, heterostructures between Bi_2Te_3 and ferromagnets have also been recently fabricated [47]. In summary, our work highlights TI-FM heterostructures, with hexagonally warped surface states, as a promising and tunable platform for realizing and probing NH phenomena.

ACKNOWLEDGMENTS

We thank A. Banerjee and A. Bose for useful discussions. M.A.R. is supported by a graduate

fellowship of the Indian Institute of Science. A.N. acknowledges support from the DST MATRICS grant (MTR/2023/000021).

AUTHOR DECLARATIONS

Conflict of Interest

The authors have no conflicts to disclose.

Author Contributions

Md Afsar Reja: Investigation (lead); Methodology (lead); Software (lead); Writing - original draft (lead). **Awadhesh Narayan:** Conceptualization (lead); Methodology (supporting); Supervision (lead); Writing - review and editing (lead).

DATA AVAILABILITY

The data that support the findings of this study are available from the corresponding authors upon reasonable request.

[1] C. M. Bender, Making sense of non-hermitian hamiltonians, *Reports on Progress in Physics* **70**, 947 (2007).

[2] Y. Ashida, Z. Gong, and M. Ueda, Non-hermitian physics, *Advances in Physics* **69**, 249 (2020).

[3] E. J. Bergholtz, J. C. Budich, and F. K. Kunst, Exceptional topology of non-hermitian systems, *Reviews of Modern Physics* **93**, 015005 (2021).

[4] K. Kawabata, K. Shiozaki, M. Ueda, and M. Sato, Symmetry and topology in non-hermitian physics, *Physical Review X* **9**, 041015 (2019).

[5] A. Banerjee, R. Sarkar, S. Dey, and A. Narayan, Non-hermitian topological phases: principles and prospects, *Journal of Physics: Condensed Matter* **35**, 333001 (2023).

[6] K. Ding, C. Fang, and G. Ma, Non-hermitian topology and exceptional-point geometries, *Nature Reviews Physics* **1** (2022).

[7] R. El-Ganainy, K. G. Makris, M. Khajavikhan, Z. H. Musslimani, S. Rotter, and D. N. Christodoulides, Non-hermitian physics and pt symmetry, *Nature Physics* **14**, 11 (2018).

[8] N. Okuma and M. Sato, Non-hermitian topological phenomena: A review, *Annual Review of Condensed Matter Physics* **14**, 83 (2023).

[9] H. Meng, Y. S. Ang, and C. H. Lee, Exceptional points in non-hermitian systems: Applications and recent developments, *Applied Physics Letters* **124** (2024).

[10] W. Heiss, The physics of exceptional points, *Journal of Physics A: Mathematical and Theoretical* **45**, 444016 (2012).

[11] T. Kato, *Perturbation theory for linear operators*, Vol. 132 (Springer Science & Business Media, 2013).

[12] A. Banerjee, R. Jaiswal, M. Manjunath, and A. Narayan, A tropical geometric approach to exceptional points, *Proceedings of the National Academy of Sciences* **120**, e2302572120 (2023).

[13] R. Jaiswal, A. Banerjee, and A. Narayan, Characterizing and tuning exceptional points using newton polygons, *New Journal of Physics* **25**, 033014 (2023).

[14] H. Hodaei, A. U. Hassan, S. Wittek, H. Garcia-Gracia, R. El-Ganainy, D. N. Christodoulides, and M. Khajavikhan, Enhanced sensitivity at higher-order exceptional points, *Nature* **548**, 187 (2017).

[15] W. Chen, S. Kaya Özdemir, G. Zhao, J. Wiersig, and L. Yang, Exceptional points enhance sensing in an optical microcavity, *Nature* **548**, 192 (2017).

[16] B. Peng, S. K. Özdemir, M. Liertzer, W. Chen, J. Kramer, H. Yilmaz, J. Wiersig, S. Rotter, and L. Yang, Chiral modes and directional lasing at exceptional points, *Proceedings of the National Academy of Sciences* **113**, 6845 (2016).

[17] M. Parto, Y. G. Liu, B. Bahari, M. Khajavikhan, and D. N. Christodoulides, Non-hermitian and topological

photronics: optics at an exceptional point, *Nanophotonics* **10**, 403 (2020).

[18] M.-A. Miri and A. Alu, Exceptional points in optics and photonics, *Science* **363**, eaar7709 (2019).

[19] T. Stehmann, W. Heiss, and F. Scholtz, Observation of exceptional points in electronic circuits, *Journal of Physics A: Mathematical and General* **37**, 7813 (2004).

[20] Y. Choi, C. Hahn, J. W. Yoon, and S. H. Song, Observation of an anti-pt-symmetric exceptional point and energy-difference conserving dynamics in electrical circuit resonators, *Nature communications* **9**, 2182 (2018).

[21] W. Zhu, X. Fang, D. Li, Y. Sun, Y. Li, Y. Jing, and H. Chen, Simultaneous observation of a topological edge state and exceptional point in an open and non-hermitian acoustic system, *Physical review letters* **121**, 124501 (2018).

[22] C. Shi, M. Dubois, Y. Chen, L. Cheng, H. Ramezani, Y. Wang, and X. Zhang, Accessing the exceptional points of parity-time symmetric acoustics, *Nature communications* **7**, 11110 (2016).

[23] L. Xiao, T. Deng, K. Wang, Z. Wang, W. Yi, and P. Xue, Observation of non-bloch parity-time symmetry and exceptional points, *Physical Review Letters* **126**, 230402 (2021).

[24] E. J. Bergholtz and J. C. Budich, Non-hermitian weyl physics in topological insulator ferromagnet junctions, *Physical Review Research* **1**, 012003 (2019).

[25] J. Cayao, Exceptional degeneracies in non-hermitian rashba semiconductors, *Journal of Physics: Condensed Matter* **35**, 254002 (2023).

[26] M. A. Reja and A. Narayan, Emergence of tunable exceptional points in altermagnet-ferromagnet junctions, *arXiv preprint arXiv:2408.04459* (2024).

[27] G. K. Dash, S. Panda, and S. Nandy, Fingerprint of non-hermiticity in ad-wave altermagnet, *Physical Review B* **111**, 155119 (2025).

[28] M. A. Reja and A. Narayan, N\’eel vector controlled exceptional contours in *p*-wave magnet-ferromagnet junctions, *arXiv preprint arXiv:2506.12434* (2025).

[29] M. Alipourzadeh, D. Afshar, and Y. Hajati, Opto- and magneto-tunable exceptional degeneracies in non-hermitian ferromagnet/*p*-wave magnet junctions, *arXiv preprint arXiv:2508.01295* (2025).

[30] M. Z. Hasan and C. L. Kane, Colloquium: topological insulators, *Reviews of modern physics* **82**, 3045 (2010).

[31] X.-L. Qi and S.-C. Zhang, Topological insulators and superconductors, *Reviews of modern physics* **83**, 1057 (2011).

[32] Y. Chen, J. G. Analytis, J.-H. Chu, Z. Liu, S.-K. Mo, X.-L. Qi, H. Zhang, D. Lu, X. Dai, Z. Fang, *et al.*, Experimental realization of a three-dimensional topological insulator, *bi2te3*, *science* **325**, 178 (2009).

[33] D. Hsieh, Y. Xia, D. Qian, L. Wray, J. H. Dil, F. Meier, J. Osterwalder, L. Patthey, J. G. Checkelsky, N. P. Ong, *et al.*, A tunable topological insulator in the spin helical dirac transport regime, *Nature* **460**, 1101 (2009).

[34] L. Fu, Hexagonal warping effects in the surface states of the topological insulator bi 2 te 3, *Physical review letters* **103**, 266801 (2009).

[35] S. Basak, H. Lin, L. Wray, S.-Y. Xu, L. Fu, M. Hasan, and A. Bansil, Spin texture on the warped dirac-cone surface states in topological insulators, *Physical Review B—Condensed Matter and Materials Physics* **84**, 121401 (2011).

[36] Z. Alpichshev, J. Analytis, J.-H. Chu, I. R. Fisher, Y. Chen, Z.-X. Shen, . f. A. Fang, and A. Kapitulnik, Stm imaging of electronic waves on the surface of bi 2 te 3:<? format?> topologically protected surface states and hexagonal warping effects, *Physical review letters* **104**, 016401 (2010).

[37] Z. Li and J. Carbotte, Hexagonal warping on optical conductivity of surface states in topological insulator bi 2 te 3, *Physical Review B—Condensed Matter and Materials Physics* **87**, 155416 (2013).

[38] Z. Li and J. Carbotte, Hexagonal warping on spin texture, hall conductivity, and circular dichroism of topological insulators, *Physical Review B* **89**, 165420 (2014).

[39] S. Saha and A. Narayan, Nonlinear hall effect in rashba systems with hexagonal warping, *Journal of Physics: Condensed Matter* **35**, 485301 (2023).

[40] D. Chowdhury, A. Banerjee, and A. Narayan, Exceptional hexagonal warping effect in multi-weyl semimetals, *Physical Review B* **105**, 075133 (2022).

[41] C. Wang and F. Yu, Effects of hexagonal warping on surface transport in topological insulators, *Physical Review B—Condensed Matter and Materials Physics* **84**, 155440 (2011).

[42] T. Choudhari and N. Deo, Effect of hexagonal warping of the fermi surface on the thermoelectric properties of a topological insulator irradiated with linearly polarized radiation, *Physical Review B* **100**, 035303 (2019).

[43] D. Ryndyk, R. Gutiérrez, B. Song, and G. Cuniberti, Green function techniques in the treatment of quantum transport at the molecular scale, in *Energy Transfer Dynamics in Biomaterial Systems* (Springer, 2009) pp. 213–335.

[44] S. Datta, *Electronic transport in mesoscopic systems* (Cambridge university press, 1997).

[45] J. Cayao and A. M. Black-Schaffer, Exceptional odd-frequency pairing in non-hermitian superconducting systems, *Physical Review B* **105**, 094502 (2022).

[46] D. C. Brody, Biorthogonal quantum mechanics, *Journal of Physics A: Mathematical and Theoretical* **47**, 035305 (2013).

[47] X. Chen, H. Wang, H. Liu, C. Wang, G. Wei, C. Fang, H. Wang, C. Geng, S. Liu, P. Li, *et al.*, Generation and control of terahertz spin currents in topology-induced 2d ferromagnetic fe3gete2| bi2te3 heterostructures, *Advanced Materials* **34**, 2106172 (2022).